High Performance Flat Plate Solar Collector

F. L. Lansing and R. Reynolds
DSN Engineering Section

This article presents briefly the potential use of porous construction to achieve efficient heat removal from a power producing solid and its new application to solar air heaters. Analytical solutions are given for the temperature distribution within a gas-cooled porous flat plate having its surface exposed to the sun's energy. The extracted thermal energy is calculated for two different types of plate transparency. The results of the analysis show the great improvement in performance obtained with porous flat plate collectors as compared with analogous nonporous types.

I. Introduction

It is technically possible to use solar-heated air to provide energy for almost any application that uses solar-heated liquids. However, it is foreseen that the most likely areas of use will be for the heating or cooling of buildings and in industrial processes such as the drying of agricultural crops and timber.

In general, solar air heaters possess the same adverse cost-temperature relationship as solar water heaters. However, they appear to cost less than water heaters because:

(1) The corrosion problems which can become serious in solar water heaters are virtually nonexistent with air heaters. This allows the use of cheaper constructional materials for reducing the cost of the collector and its accessories.

(2) The leakage of air from the ducts or the heater connection does not present a serious problem. A hermetic system is not essential as when using water as the working fluid. This presents another potential cost reduction in installation and maintenance.

(3) Solar air heaters are lighter in weight and less complex than solar water heaters. This again reduces the inherently high cost of "add on" systems if solar collectors are integrated into a building structure.

On the other hand, solar air heaters have relatively high fan power requirements and without careful design the duct costs can also be high. Also, storage of energy with a solar air heating system presents problems different from storage with solar water heating where the actual heat transfer fluid can generally be used as the storage medium. The storage material to be chosen should be of

low cost, high thermal capacitance, and be able to exchange heat with the air with small heat transfer surface area.

Though it can be concluded that there exists an economic potential for using air as the working medium in solar collectors, the state of the art remains a technical achievement awaiting commercial exploitation. A solar air heater that provides effective heating and combines high power density with compactness of heat exchange surface is exemplified by the porous flat plate solar collector, which is the main subject of this article.

Porous materials have become increasingly attractive for application in high temperature heat exchangers. The present new application of porous heat transfer in a plate subjected to solar radiation is exceptionally effective in both heating the working fluid and improving the absorptive characteristics of the plate. The high effectiveness of the heat exchange mechanism is mainly due to the intimate contact in the interstices between the gas particles and the porous plate, as will be explained in the next sections.

II. Collector Description

The high performance flat plate solar collector utilizes air as the heat transfer fluid and is shown schematically in Figs. 1, 2, and 3. It is composed mainly of a metallic matrix whose mesh size and porosity depend on the required performance and acts as the absorber plate in a conventional flat plate solar collector. The porosity of the matrix surface behaves as a large set of cavity radiators (black bodies) whose absorptivity greatly exceeds that of a regular solid surface. One or two sheets of glass are mounted on top of the matrix, allowing a space for the air flow passage. The space between the glazings, if more than one sheet is used, may be evacuated to reduce the thermal convection and conduction losses. Also, the matrix surface can be coated by a "selective" material to reduce the outward long wave radiation losses. It should be pointed out that the use of vacuum and selective coating are not the main points behind the high performance obtained in the present work but rather the new heat exchange mechanism in a porous material. The comparison will always be made between two identical collectors, one with a porous plate, and the other without. The cold air flows through the matrix plate and exchanges heat with its thermally stratified layers. The heat exchange mechanism may take either one of the three patterns shown in Figs. 1, 2, and 3, depending on the direction of air flow with respect to the matrix thermal stratification.

To show, in a simple manner, the important features of the novel porous plate solar collector, the one-dimensional flow pattern illustrated in Fig. 1 is found to be the best candidate pattern for the present work comparison. The flow pattern in Fig. 2 is subject to reversing flow effects due to hot air buoyancy and it possesses a complex flow regime. Also, the flow pattern in Fig. 3 is excluded from the present discussion since it needs a more complicated, two-dimensional study.

III. Basic Assumptions and Analysis

The basic assumptions that are used in the steady state thermal analysis can be listed as follows:

(1) Thermal, physical, and transport properties of the matrix plate and the fluid (air) are constant with temperature and uniform over the entire collector area.

(2) Heat conduction and fluid flow are one dimensional in a direction perpendicular to the bounding surfaces of the matrix.

(3) Temperatures of the fluid and the matrix pores are equal at any position within the plate. This assumption may not be very accurate for matrix heat exchangers (regenerators) with large fluid flow rates. However, this idealization in the mathematical model is still considered essential in most of the analytical studies of transpiration-cooled matrices as described in Refs. 1–5.

(4) Heat losses to the ambient air by convection and radiation are only from the top surface of the matrix plate facing the solar radiation. No allowance is made for the bottom surface losses.

Based on these idealizations, a segment of the collector matrix of thickness dy and at a depth y from the top surface facing the sun is analyzed as shown in Fig. 4.

The steady state temperature distribution is determined by solving the heat balance equation of the collector segment, which is written as: The sum of the net rates of heat conduction, increase of fluid energy content, and internal heat absorption is equal to the rate of energy storage, i.e.,

$$K_e \frac{d^2T}{dy^2} + G_f C_f \frac{dT}{dy} + Q_{in}(y) = 0 \qquad (1)$$

Equation (1) is the system differential equation and is solved for the following two extreme cases:

Case 1: an opaque surface matrix with total absorption of the sun's energy at the top surface. This is a case of close packed meshes whose internal heat absorption, Q_{in}, is treated as a surface property.

Case 2: a diathermanous matrix (semitransparent to radiation) with successive absorption of the solar energy within the matrix depth. This is a case of loose packed semitransparent matrix with relatively large mesh size whose internal heat absorption, Q_{in}, is treated as a bulk property.

The temperature profile in each of the above cases is analyzed as follows:

Case 1: An Opaque Matrix Surface: for total absorption of solar irradiancy at the surface ($y = 0$), then

$$Q_{in}(y) = 0 \qquad \text{for } y > 0 \tag{2}$$

and Eq. (1) is reduced to

$$K_e \frac{d^2T}{dy^2} + G_f C_f \frac{dT}{dy} = 0 \tag{3}$$

with its general solution given by

$$T = A_1 + B_1 \exp\left(\frac{-G_f C_f y}{K_e}\right) \qquad \text{for } 0 \leq y \leq L \tag{4}$$

where A_1 and B_1 are arbitrary constants to be determined from the boundary conditions. Equation (4) is only applicable to matrix (or fluid) temperatures within the range $0 \leq y \leq L$.

The boundary conditions of case 1 are set as follows:

(1) At the fluid entry section ($y = L$), the rise in fluid energy is equal to the rate of heat conduction from the matrix surface.

(2) At the fluid exit section ($y = 0$), the first law of thermodynamics necessitates that the net absorbed solar energy (the absorbed solar energy minus the heat losses to the environment) equals the rise in fluid energy from its entry up to the exit section.

The temperature distribution within the plate is thus given by the exponential form:

$$T = T_{in} + \left[\frac{\alpha_p \tau_g q - U_e(T_{in} - T_a)}{[G_f C_f + U_e]}\right] \exp\left(\frac{-G_f C_f y}{K_e}\right) \tag{5}$$

and is sketched in Fig. 5. The temperature distribution is dependent on the conductivity K_e and the thickness L. However, the fluid temperature rise across the collector is independent of K_e and L and is given by:

$$[T(0) - T_{in}] = \left[\frac{\alpha_p \tau_g q - U_e(T_{in} - T_a)}{(G_f C_f + U_e)}\right] \tag{6}$$

The useful heat gain Q_u per unit area is then expressed as

$$\begin{aligned} Q_u &= G_f C_f [T(0) - T_{in}] \\ &= [\alpha_p \tau_g q - U_e(T_{in} - T_a)]\left(\frac{G_f C_f}{G_f C_f + U_e}\right) \end{aligned} \tag{7}$$

Case 2: A Diathermanous Matrix (Semitransparent to Radiation): in this case, the matrix absorbs incident solar radiation not only at the top surface but at successive depths also. The internal heat absorbed per unit volume, $Q_{in}(y)$, is derived using Beer's Law for diathermanous materials and is given by

$$Q_{in}(y) = a\tau_g q \exp(-ay) \tag{8}$$

where a is the extinction coefficient of the plate. The system differential equation, Eq. (1), is reduced to

$$K_e \frac{d^2T}{dy^2} + G_f C_f \frac{dT}{dy} + a\tau_g q \exp(-ay) = 0 \tag{9}$$

whose general solution is given by:

$$T = A_2 + B_2 \exp\left(\frac{-G_f C_f y}{K_e}\right) + \frac{q\,\tau_g \exp(-ay)}{(G_f C_f - K_e a)} \qquad \text{for } 0 \leq y \leq L \tag{10}$$

where A_2 and B_2 are arbitrary constants to be determined from the boundary conditions. Equation (10) is only applicable to matrix (or fluid) temperatures within the range $0 \leq y \leq L$.

The boundary conditions for case 2 are set as follows:

(1) At the fluid entry section ($y = L$), the rise in fluid energy is equal to the rate of heat conduction from the matrix surface plus the leaving unabsorbed radiation.

(2) At the fluid exit section ($y = 0$), the first law of thermodynamics necessitates that the net absorbed solar energy (the absorbed solar energy minus the

heat losses to the environment) equals the rise in fluid energy from its entry up to the exit section.

The temperature distribution within the diathermaneous matrix is thus given by

$$T = T_{in}\left[\frac{q\,\tau_g(1-\exp(-aL)) - U_e(T_{in}-T_a)}{(U_e+G_fC_f)}\right] \times \exp\left(\frac{-G_fC_fy}{K_e}\right) + \frac{q\,\tau_g\left[\exp(-ay) - \exp\left(\frac{-G_fC_fy}{K_e}\right)\right]}{(G_fC_f - K_ea)} \quad (11)$$

and is sketched in Fig. (6). The maximum fluid temperature rise is written as

$$[T(0) - T_{in}] = \left[\frac{q\,\tau_g(1-\exp(-aL)) - U_e(T_{in}-T_a)}{(U_e+G_fC_f)}\right] \quad (12)$$

which is independent of the conductivity K_e of the matrix. The useful heat gain Q_u can be derived using Eq. (12) as

$$Q_u = G_fC_f\,[T(0) - T_{in}] = [\tau_g q(1-\exp(-aL)) - U_e(T_{in}-T_a)]\left(\frac{G_fC_f}{G_fC_f+U_e}\right) \quad (13)$$

which is similar to that obtained in Eq. (7) except that the plate absorptivity (α_p) is now replaced by its equivalent form $(1-\exp(-al))$.

The temperature profile within the porous structure is plotted for the above two cases as shown in Figs. 5 and 6, and at some selected values for G_f, C_f, K_e, L, q, a, and τ_g. For an opaque surface, the temperature decreases monotonically from the absorber surface as shown in Fig. 5.

In the diathermanous matrix, the temperature experiences a maximum value at some point inside the matrix due to the successive absorption of the sun's energy and the energy transported away by the fluid. It is desirable, from the thermal stresses view point, to have a uniform matrix plate temperature distribution. To satisfy this criteria the operating conditions should result in a higher value for the wall temperature $T(L)$ at the fluid entry section. The latter is promoted by using a high thermal conductivity, K_e, a small plate thickness, L, and a small air mass flux, G_f.

IV. Comparison With a Nonporous (Solid) Flat Plate Collector

The conventional, solid flat plate solar collector that uses air as the working medium is sketched in Fig. 7. The absorber plate is provided with side fins to enhance the heat conductance rate to the air blowing underneath it. The useful heat gain expression is presented in detail in several literature sources (Ref. 6, for example) and is rewritten for reference as

$$Q_{u\ \text{solid flat plate}} = \{\alpha_p\,\tau_g\,q - U_e(T_{in}-T_a)\} \times \frac{G_fC_f}{U_e}\left\{1-\exp\left(-\frac{U_eU_{pf}}{G_fC_f(U_e+U_{pf})}\right)\right\} \quad (14)$$

where U_{pf} is the conductance coefficient between the plate and the adjacent working fluid (air). The rest of the parameters bear the same meaning as used before.

The present analysis of the high performance solar collector that uses a porous flat plate with a working fluid flowing through the interstices, yields an analogous expression for its useful heat gain, and it is given in Eqs. 7 and 13 as

$$Q_{u\ \text{porous flat plate}} = \{\alpha_p\,\tau_g q - U_e(T_{in}-T_a)\}\frac{G_fC_f}{(G_fC_f+U_e)} \quad (15)$$

It can be concluded that for the same optical properties (α_p, τ_g), solar radiation intensity, q, and the loss coefficient from the plate surface to the environment U_e, the performance of a porous collector depends exclusively on the product of the fluid mass flux times its specific heat (G_fC_f), while that of the solid type depends on the conductance coefficient U_{pf} as well as the product G_fC_f. Table 1 presents the results of a numeric comparison between the two types and is constructed from the following assumed operating conditions:

Solar radiation intensity q = 678 kcal/h-m² (250 BTU/h-ft²)

Ambient air temperature T_a = 10°C (50°F)

Inlet air temperature T_{in} = 23.89°C (75°F)

Matrix plate absorptivity $\alpha_p = 0.9$ (this corresponds to an extinction coefficient of 0.906 cm^{-1} (27.63 ft^{-1}) for 2.54-cm (1-in.) thickness diathermaneous material)

Matrix plate emissivity $\epsilon_p = 0.9$

Glass cover transmissivity $\tau_g = 0.9$

Loss coefficient between plate surface and environment $U_e = 5.86$ kcal/h-m^2 °C (1.2 BTU/h-ft^2 °F)

Air Specific heat $C_f = 0.24$ kcal/kg °C (0.24 BTU/lb °F)

Matrix porosity $p = 0.8$

the solid plate to air conductance coefficient U_{pf} is given by the approximate formula

$$U_{pf} \approx 4.883\,(1.0 + 0.248\,V)\ \text{kcal/h-m}^2\ ^\circ\text{C}$$

where V is the air velocity in km/h.

The above operating conditions were abstracted from the experimental results of flat plate solar collectors to yield a practical evaluation of the present comparison. The efficiency results are plotted as shown in Fig. 8.

It is evident from Fig. 8 that a much higher performance can be obtained with a porous flat plate collector relative to the analogous solid type. This is due to the fact that the heat transfer mechanism between the matrix plate and the air in the interstices is far more effective in making their temperatures equal. This means that the porous flat plate heat exchanger is in effect working with an extremely larger value of the plate to fluid conductance U_{pf}, relative to the nonporous type. Their performance can be identical only at the "no flow" condition, and both of them yield

$$\lim_{G_f \to 0} [T(0) - T_{in}] = \{\alpha_p \tau_g q - U_e(T_{in} - T_a)\} \frac{1}{U_e} \tag{16}$$

which is the highest temperature difference that could be attained by any of them.

The above calculations do not consider other factors such as the variation of the loss coefficient U_e and plate to fluid conductance U_{pf} with operating temperatures, and the potential improvement of optical absorptivity brought by a black body type absorbing surface for the porous material. The efficiency value obtained from the present high performance collector still leads with a sizable margin at all operating conditions. As an example, for a high efficiency collector application, Table 1 indicates that with an air mass flux of 4880 kg/h-m^2 (1000 lb/h-ft^2), which corresponds to an air velocity of approximately 4 km/h (2.5 mi/h), the efficiency improvement is 59 percent over a conventional solid type, however, the temperature gain is very little. On the other hand, for a higher temperature application where the air is heated by 16°C (29°F), the corresponding mass flux is approximately 98 kg/h-m^2 (20 lb/h-ft^2), and an improvement in efficiency over a conventional type of 84 percent could be obtained. Preliminary evaluation of this high performance solar collector indicates that it is capable of working with liquid phase heat exchange fluids as well as gases. Future work will address the application of this configuration of collector to liquid and boiling type heat exchange fluids.

Definition of Symbols

a extinction coefficient

C_f fluid specific heat

G_f fluid mass flux (Flow rate per unit area)

K_e "effective" matrix conductivity

L matrix plate thickness

p porosity (pore volume/total volume)

q solar radiation intensity

Q_{in} internal heat generation per unit volume

T temperature

U_e "effective" heat loss coefficient between matrix and ambient

U_{pf} solid plate to fluid conductance coefficient

V velocity

y distance measured from the top surface facing the sun

α_p plate absorptivity

τ_g glass cover transmissivity

ϵ_p plate emissivity

References

1. Burch, D. M., and Peavy, B. A., "Transient Temperature Distribution in Heat–Generating–Transpiration Cooled Tubes and Plates," *Journal of Heat Transfer, ASME Trans. Series C*, Vol. 97, Aug. 1975.

2. Rohsensow, W. M., and Hartnett, J. P., *Handbook of Heat Transfer*. McGraw Hill Book Co., N.Y., 1973, Ch. 3.

3. Schneider, P. J., "Temperatures and Thermal Stresses in Transpiration–Cooled Power Producing Plates and Tubes," *Jet Propulsion*, Vol. 27, Aug. 1957, pp. 882–889.

4. Schneider, P. J., "Numerical Method for Porous Heat Sources," *Journal of Applied Physics*, Vol. 24, No. 3, March 1953, pp. 271–274.

5. Green, L., "Gas Cooling of a Porous Heat Source," *Journal of Applied Mechanics, TRANS ASME*, Vol. 19, No. 2, 1952, pp. 173–178.

6. Whillier, A., "Design Factors Influencing Solar Collector Performance," in *Low Temperature Engineering Application of Solar Energy*, ASHRAE Publications, 1967, Ch. III, pp. 27–40.

Table 1. Comparison between a porous and a nonporous flat plate solar air heater

G_f, kg/h-m² (lb/h-ft²)	Useful temperature rise $(T(0) - T_{in})$, °C (°F)		Thermal efficiency, %		Improvement in efficiency, %
	Porous	Nonporous (solid)	Porous	Nonporous	
0	79.86 (143.75)	79.86 (143.75)	0.00	0.00	0
24.4 (5)	39.93 (71.88)	29.23 (52.62)	34.50	25.26	37
48.8 (10)	26.62 (47.92)	16.31 (29.36)	46.00	28.19	63
97.6 (20)	15.97 (28.75)	8.66 (15.60)	55.20	29.95	84
244 (50)	7.26 (13.07)	3.64 (6.55)	62.73	31.46	99
488 (100)	3.80 (6.84)	1.89 (3.40)	65.71	32.61	102
976 (200)	1.95 (3.51)	0.99 (1.78)	67.32	34.28	96
2440 (500)	0.79 (1.42)	0.44 (0.80)	68.32	38.23	79
4880 (1000)	0.39 (0.71)	0.25 (0.45)	68.66	43.06	59

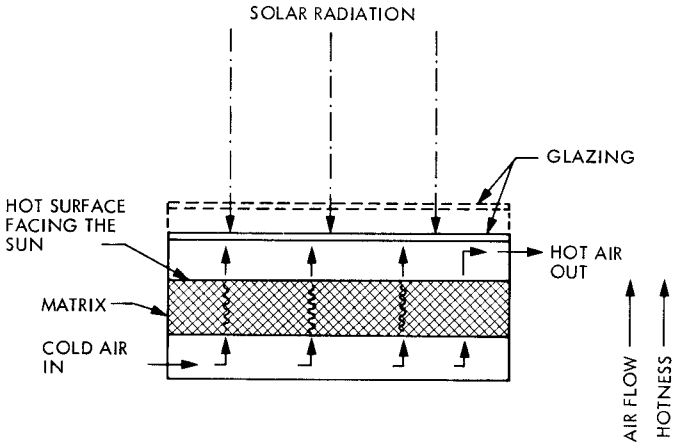

Fig. 1. Upward flow of cold air towards the direction of hotter layers of the matrix

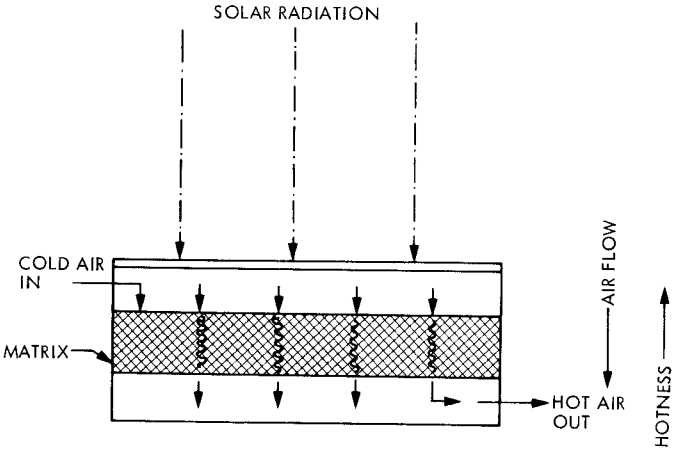

Fig. 2. Downward flow of cold air against the direction of hotter layers of the matrix

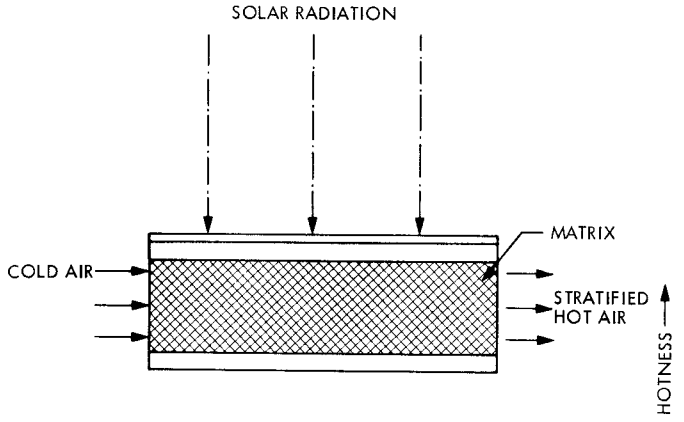

Fig. 3. Lateral flow of cold air across the direction of hotter layers of the matrix

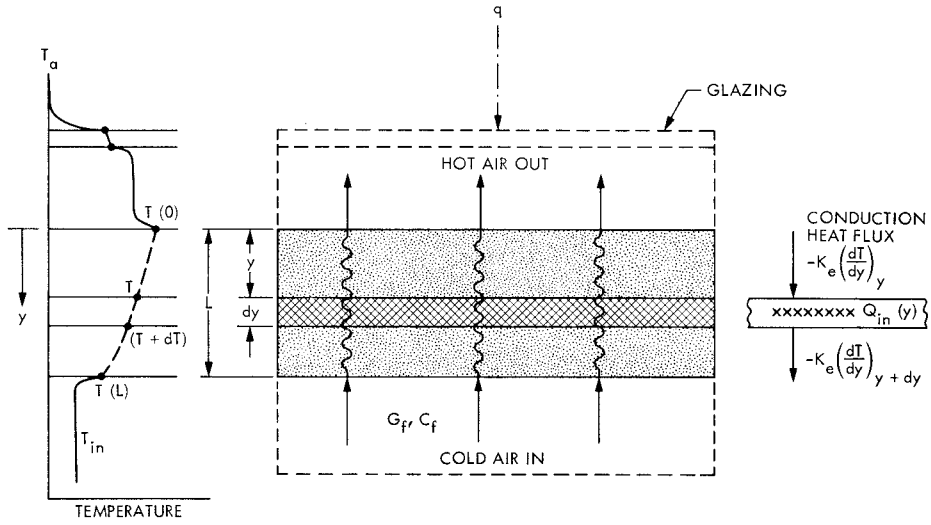

Fig. 4. Heat balance of an element of matrix plate

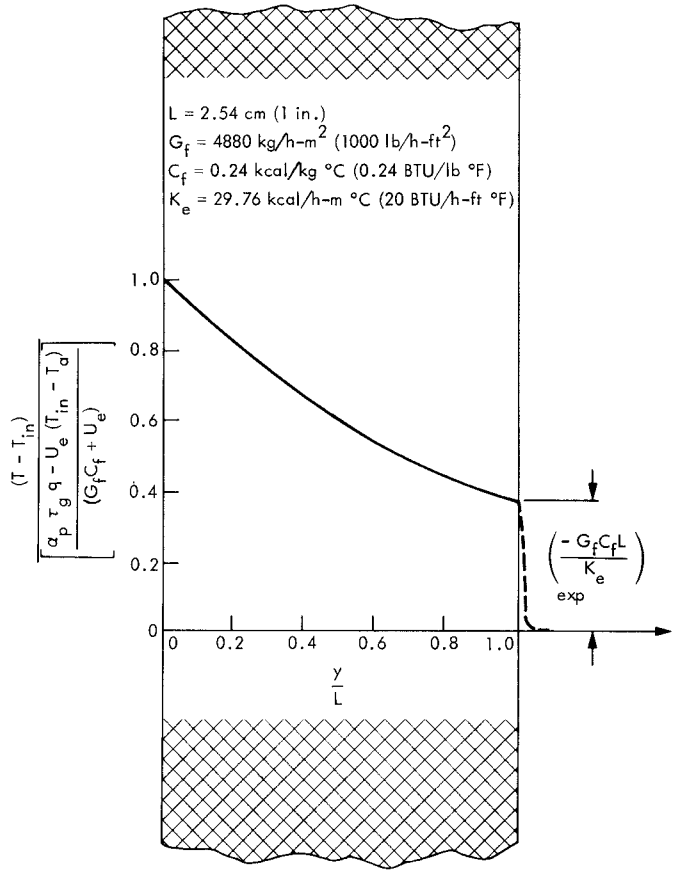

Fig. 5. Matrix and fluid temperature profile for an opaque matrix surface

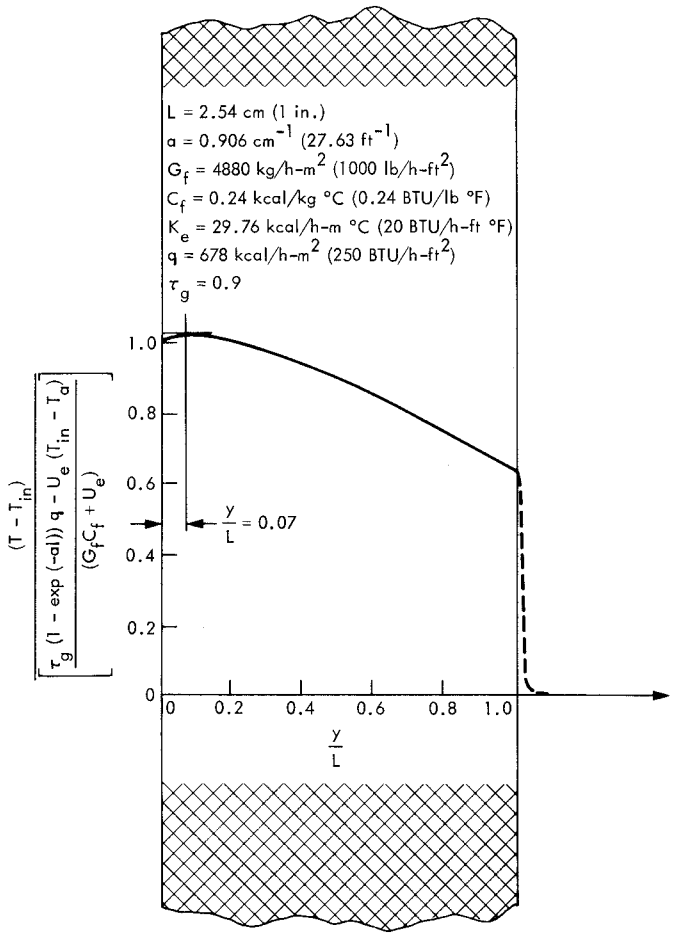

Fig. 6. Matrix and fluid temperature profile for a diathermaneous matrix

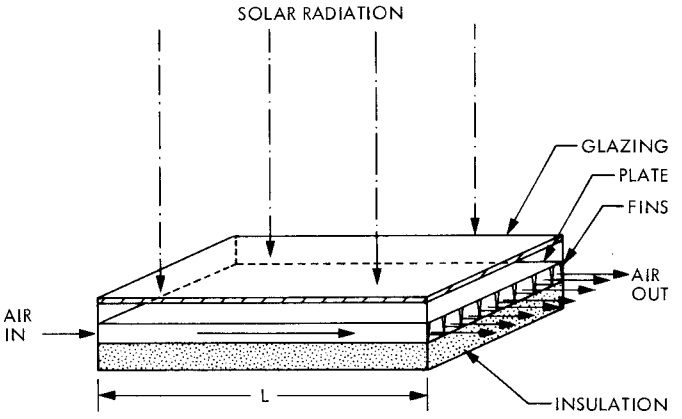

Fig. 7. Nonporous, flat plate solar air heater

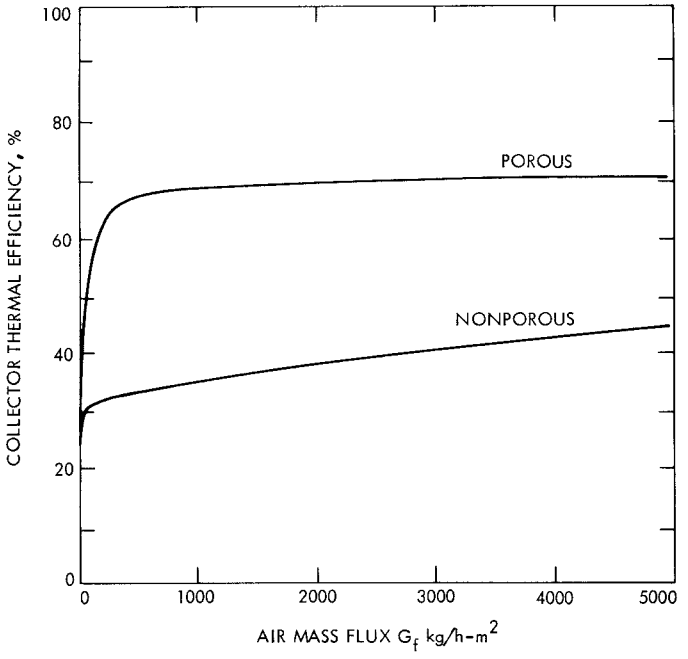

Fig. 8. Results of the numerical example to compare the thermal efficiency between a porous and nonporous collector